

Mesoporous TiO₂ and copper-modified TiO₂ nanoparticles: A case study

R. Ajay Kumar¹, V.G. Vasavi Dutt¹, and Ch. Rajesh^{1,2a}

¹ Advanced Functional Materials Research Centre, Koneru Lakshmaiah Education Foundation, Vaddeswaram, Guntur, Andhra Pradesh 522502, India

² Department of Physics, Koneru Lakshmaiah Education Foundation, Vaddeswaram, Guntur, Andhra Pradesh 522502, India

Received: 21 August 2017 / Revised: 16 November 2017

Published online: 16 February 2018 – © Società Italiana di Fisica / Springer-Verlag 2018

Abstract. In this paper we report the synthesis of mesoporous titanium dioxide (M-TiO₂) nanoparticles (NPs) and copper (Cu)-modified M-TiO₂ NPs by the hydrothermal method at relatively low temperatures using cetyltrimethylammonium bromide (CTAB) as a template. In order to get ordered spherical particles and better interaction between cationic and anionic precursor, we have used titanium isopropoxide (TTIP) as titanium source and CTAB as surfactant. The process of modification by copper to M-TiO₂ follows the impregnation method. The change in structural and optical properties of NPs were estimated using different characterization techniques like X-ray diffraction, field emission scanning electron microscopy, Brunner-Emmett-Teller curve and UV-Vis absorption analysis. M-TiO₂ and Cu-modified M-TiO₂ exhibit pure anatase crystalline phase and shows no evidence of CuO formation. Nitrogen adsorption-desorption hysteresis reveals that the material is mesoporous. Several samples synthesized at different process temperature were further studied in order to make them suitable for a wide range of applications.

1 Introduction

Titanium dioxide (TiO₂) material has been widely used as photo-catalysts, sensors, for hydrogen storage, photovoltaic and energy applications [1]. Anatase TiO₂ is a promising material as negative electrode for Li-ion batteries because of its inexpensiveness, structural stability, non-toxicity to the environment and high discharge voltage plateau (at 1.7 eV) [2]. TiO₂ nanoparticles (NPs) of different morphology are widely used as photo-anode material in dye-sensitized solar cells to increase their photo-conversion efficiency [3]. TiO₂ mainly exists in three crystalline polymorphs: anatase, rutile and brookite. These three polymorphs have different crystalline structures, anatase and rutile have tetragonal structure whereas brookite is orthorhombic. TiO₂ shows high reactivity and chemical stability under ultraviolet light, whose energy exceeds the band gap of 3.3 eV in the anatase crystalline phase TiO₂, thus limiting the reactivity in the visible range [1]. Many studies were carried out to decrease its band gap with lower rate of recombination of the electron-hole pair. It can be achieved by proper doping of metal ions, surface modification and dye photosensitization of TiO₂ surface [4,5]. TiO₂ can be synthesized via various methods: hydrothermal [6], solvothermal [7], electrodeposition [8], sonochemical [9] and sol-gel [10] methods. Hydrothermal process is preferable because it is low cost and simple.

Preparation of different TiO₂ micro and nano structures of various morphologies has drawn a great attention of many researchers because of its photo-catalytic property. TiO₂ mesoporous material is of particular interest for the treatment of environmental pollutants because they have larger specific surface area and pore size making it an ideal material as catalyst. Wang *et al.* [11] synthesized mesoporous TiO₂ via a hydrothermal process using cetyltrimethylammonium bromide (CTAB) as template and compared the photo-catalytic activity of synthesized mesoporous TiO₂ with commercial P25 for degradation of methyl orange. Tan *et al.* [12] reported the synthesis of layered TiO₂ nanostructures using the hydrothermal method which involves the hydrolysis of the Ti precursor in the presence of tetramethylammoniumhydroxide (TMAH) as capping agent. Wang *et al.* [13] prepared Cu-doped mesoporous TiO₂ by the hydrothermal method and showed an enhancement of absorption in the visible-light region, thus increasing the photo-catalytic activity. They explained the enhancement of photo-catalytic behaviour through the stabilization of copper dispersed in TiO₂.

^a e-mail: rajesh8112@gmail.com

Yoong *et al.* [14] showed the advantage of copper doping to the photo-catalyst TiO_2 for hydrogen generation. In this paper [14] they incorporated copper into TiO_2 using two methods: one is by complex precipitation and the other by the wet impregnation method with different copper loading concentrations. The band gap narrowing with copper was estimated and the influence of other parameters on the photo-catalytic activity for hydrogen generation was explained.

In the present work, pure mesoporous TiO_2 (M- TiO_2) and Cu-modified M- TiO_2 particles are prepared via the hydrothermal process by varying the process temperature and copper modification by concentration. In order to get ordered spherical particles we need to have better interaction between cationic and anionic precursor. As far as, our knowledge goes, till now there are no such reports wherein a combination of TTIP as titanium source and CTAB as surfactant has been used. Their structural properties are studied using X-ray diffraction (XRD), field emission - scanning electron microscopy (FE-SEM) and Brunner-Emmett-Teller (BET) characterization techniques. Their optical properties like absorption and band gap energy values are estimated from the results of UV-Vis spectrophotometry. Naming is given as MT-100, MT-130 and MT-150 for the samples M- TiO_2 synthesized at the different process temperatures 100, 130 and 150 °C, respectively. CMT-100, CMT-130 and CMT-150 represent Cu-modified M- TiO_2 at 0.1 at% copper concentration with the different process temperatures 100, 130 and 150 °C.

2 Experimental procedure

All the chemicals were analytical grade and can be used without further purification. TiO_2 NPs were prepared via hydrothermal process using the precursor titanium isopropoxide (TTIP, 97%, Sigma Aldrich), a cationic surfactant cetyltrimethylammonium bromide (CTAB) obtained from Sigma Aldrich is used as template.

2.1 Hydrothermal method

1 gm of CTAB is added to ethanol and mixed continuously for 3 hours. Then TTIP is added such that the final molar ratio of the solution is 1:0.3:50 (Ti:CTAB:Ethanol) and stirred continuously for 3 hours. The contents were transferred to PTFE line autoclave (100 mL capacity) and maintained at 100, 130, and 150 °C for 36 hours. After cooling to room temperature, the obtained gel is centrifuged and washed with ethanol for 3 times. The sample is dried in hot air oven at 100 °C for 12 hours. The precipitate is ground and crushed in mortar to get fine nanopowder. The powdered sample is calcinated at 500 °C for 3 hours.

2.2 Copper modification using the impregnation method

With the impregnation method, copper-modified mesoporous TiO_2 particles were obtained by mixing the as-synthesized particles into a beaker containing an aqueous solution of $\text{CuCl}_2 \cdot 2\text{H}_2\text{O}$ with copper concentration of 0.05, 0.1, and 0.3%. The mixture is stirred well for 1 hour maintaining at ~ 70 °C after cooling, the sample is washed with de-ionized water and filtered. It is dried in hot air oven for 6 hours at 100 °C to get Cu-modified M- TiO_2 , which is pale brown in colour.

Phase identification of the as synthesized M- TiO_2 and Cu-modified M- TiO_2 nanoparticles were carried on Bruker D8 advance with Cu K_α radiation ($\lambda = 1.5405$ Å), with a scan rate of 4.0 degree per min, and an operating voltage of 40.0 KV and current of 30.0 mA. Morphological studies were performed with the help of field emission scanning electron microscope (FE-SEM) using a SU1510, Hitachi model at EHT = 30 KV. The surface analysis (BET) was performed on 11-2370 Gemini.

3 Results and discussions

3.1 X-ray diffraction

X-ray diffraction (XRD) patterns of pure and Cu-modified mesoporous TiO_2 were compared with the standard anatase diffraction pattern as shown in figs. 1(a) and (b), respectively. The peaks at $2\theta = 25.30^\circ, 36.95^\circ, 37.79^\circ, 38.56^\circ, 48.03^\circ, 53.89^\circ, 55.06^\circ, 62.69^\circ, 68.76^\circ, 70.29^\circ$ and 75.05° are assigned to 101,103, 004, 112, 200, 105, 211, 204, 116, 220 and 215 planes attributed to the anatase phase of TiO_2 which is also in good agreement with standard data (JCPDS No. 04-014-8515). A similar XRD pattern was also obtained for Cu-modified mesoporous TiO_2 particles. Upon analysing both the patterns, it was found that in copper-modified TiO_2 the value of the lattice constant is slightly higher when compared with M- TiO_2 . This is can be attributed to strains induced due to the incorporation of copper in the TiO_2 lattice. It is observed that some higher-order peaks are not well resolved indicating the presence of small-sized particles.

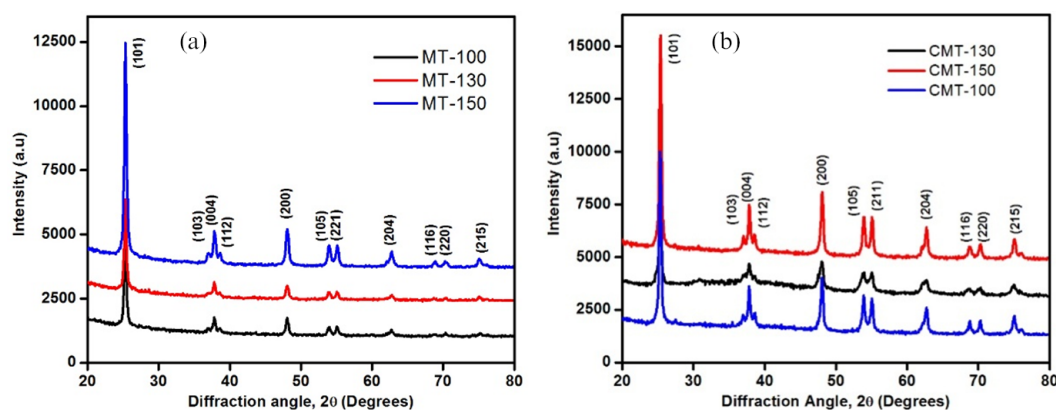


Fig. 1. XRD patterns of mesoporous (a) pure TiO_2 and (b) Cu-modified TiO_2 with different process temperatures.

With the increase in process temperature, the crystallinity also increases, which is attributed to the sharpness of the peak. The crystallite size was calculated from broadening of the main peak, *i.e.* FWHM by Scherrer's formula,

$$D = 0.9\lambda/\beta \cos \Theta \text{ nm},$$

where β is the full width at half maximum (FWHM) of the diffraction peak, λ is the X-ray wavelength (nm) and Θ is the diffraction angle. The highest-intensity peak at $2\theta = 25.48^\circ$ ((101) orientation) is considered for calculating the size of the particles. For copper-doped mesoporous TiO_2 also the particle size was calculated in a similar manner. The lattice parameters were calculated for pure and copper-modified M- TiO_2 particles and were found to be $a = 3.754 \text{ \AA}$ and $c = 9.332 \text{ \AA}$ for pure and $a = 3.867 \text{ \AA}$ and $c = 9.424 \text{ \AA}$ for copper-modified M- TiO_2 particles.

The calculated crystallite size of mesoporous TiO_2 synthesized with different process temperatures 100, 130 and 150°C are 18 ± 0.7 , 24 ± 0.4 and 24 ± 0.8 nm, respectively. Figure 1(b) shows the XRD patterns of Cu-modified TiO_2 synthesized at different temperatures 100, 130 and 150°C . The calculated crystallite size using Scherrer's formula for the above-mentioned samples are 21 ± 0.6 , 26 ± 0.4 and 26 ± 0.9 nm, respectively. The patterns show the existence of the anatase crystalline phase without any extra impurity peak even after Cu modification.

3.2 Field emission: Scanning electron electroscopy

The FE-SEM images of mesoporous TiO_2 synthesized at the different process temperatures 100, 130 and 150°C are shown in figs. 2(a)–(f). The images show the presence of ordered spherical particles with size of approximately 44 ± 0.3 nm. The distributions of spherical particles are uniform for nanoparticles synthesized with a process temperature of 100°C . When the hydrothermal process temperature (130°C) is increased, there is an improvement in the growth and agglomeration of the particles. The size of the spherical particles (~ 51 nm) has also increased with respect to that of particles synthesized at 100°C . With further increasing the synthesis temperature to 150°C , more agglomeration occurs in TiO_2 particles. The particle size of nanoparticles prepared at 150°C is ~ 58 nm and show an improvement in crystal growth, *i.e.* the high temperature is responsible for the formation of bigger TiO_2 particles. The particle sizes obtained from FE-SEM analysis are larger compared to those obtained from the XRD analysis. XRD provides an estimate of crystallite size, whereas FE-SEM provides the particle size. In general the particle is made up of a large number of crystallites. The formation of fine particles with homogenous distribution may be attributed to the enhanced interaction between cationic CTAB and anionic Ti precursor during the reaction process.

3.3 BET analysis

Figure 3 shows the nitrogen adsorption desorption isotherm of mesoporous TiO_2 prepared at various process temperatures, 100, 130 and 150°C , to evaluate pore structure and size. The materials exhibit type-IV isotherms with a pronounced capillary condensation stepping between 0.6 and 0.9p/p₀ which shows the presence of mesoporous structures [15]. The pore volume and pore diameter of mesoporous TiO_2 increased with increasing process temperature as shown in table 1. These excellent physico-chemical characteristics of mesoporous TiO_2 will be an advantage for photo-catalytic applications as they enhance the adsorption properties of TiO_2 . There is no shift of capillary condensation with increase of process temperature. But there is an increase in the surface area of MT-150 which reveals that at higher process temperature, the particle size decreases, *i.e.* the surface area is consistent with the size of the particle through FESEM images of MT-100, MT-130 and MT-150. From the BET analysis, it is observed that the pore diameter of MT-130 is greater when compared with that of MT-100 and MT-150. Hence it can be concluded that MT-130 carries a lower number of pores than MT-100 and MT-150.

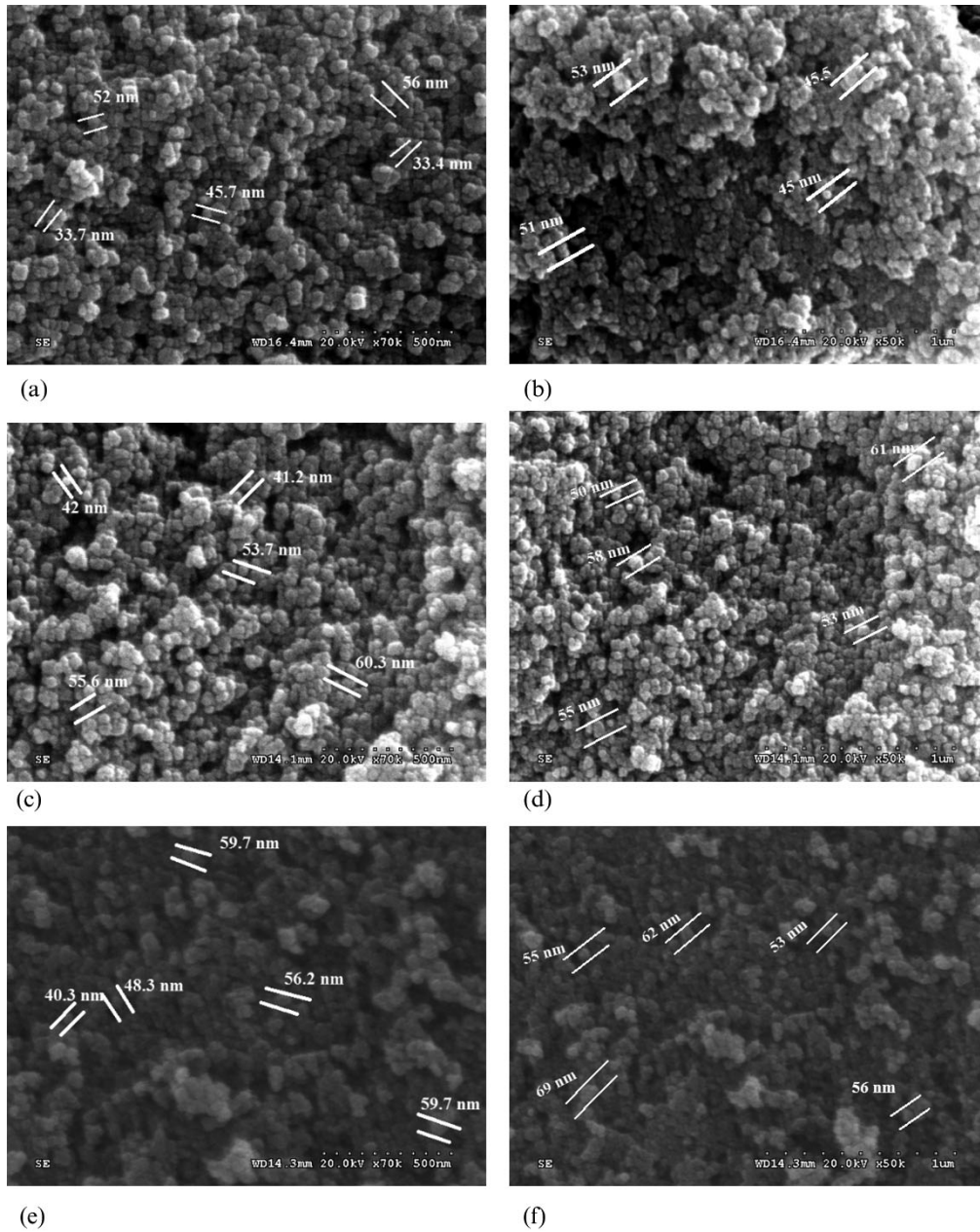


Fig. 2. ((a), (b)) Mesoporous TiO₂ synthesized with process temperature 100 °C, ((c), (d)) with process temperature 130 °C and ((e), (f)) with process temperature 150 °C.

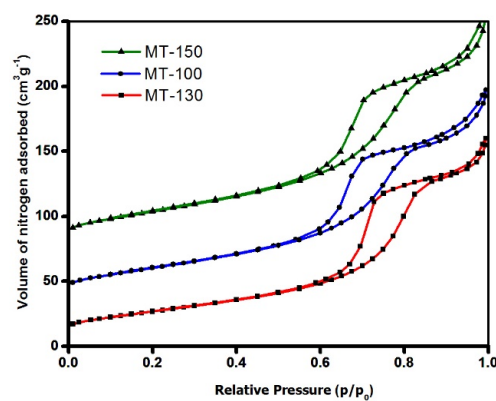


Fig. 3. Nitrogen adsorption-desorption isotherm of (a) MT-100, (b) MT-130 and (c) MT-150.

Table 1. Textural properties of M-TiO₂ synthesized at different process temperatures, 100, 130 and 150 °C.

Material	Specific surface area (m ² /g)	Pore volume (Cm ² /g)	Pore size (Å)
MT-100	97.56	0.27	189.91
MT-130	111.26	0.19	305.62
MT-150	123.38	0.33	257.95

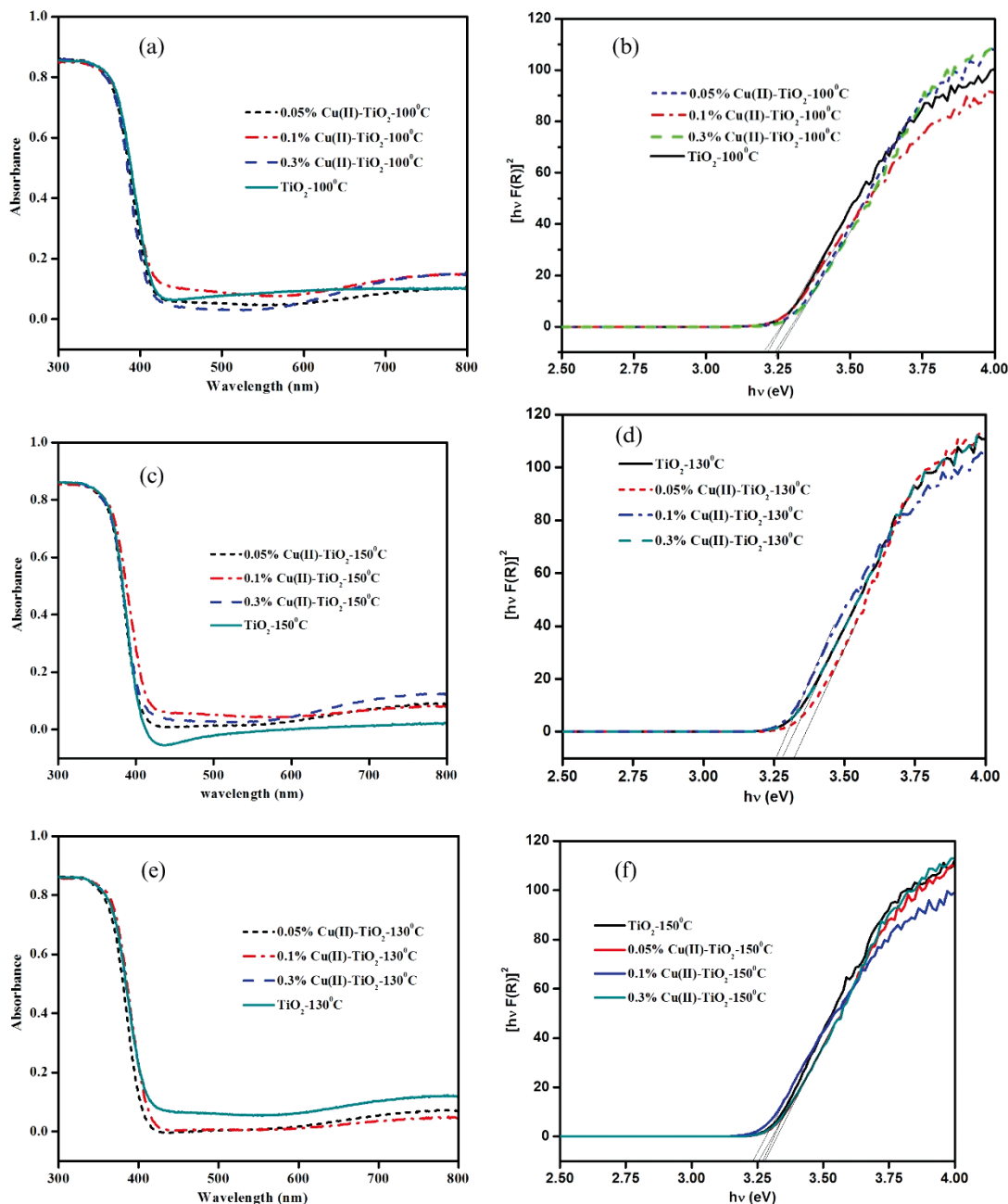


Fig. 4. UV-Vis absorption spectra ((a), (c), (e)) and band gap plot ((b), (d), (f)) of mesoporous pure TiO₂ and Cu-TiO₂ at different concentrations 0, 0.05%, 0.1% and 0.3%, respectively.

3.4 UV-Vis analysis of pure and Cu-modified TiO₂

Mesoporous pure TiO₂ and Cu-modified TiO₂ at different concentrations were characterized using diffused-reflectance UV-Vis spectroscopy as shown in fig. 4. Band gap energy values are calculated by representing the reflectance with

Table 2. Band gap values of TiO₂ and Cu-modified TiO₂ synthesized at different process temperatures.

Concentration of Cu modification to TiO ₂ (at%)	Cu-TiO ₂ different process temperatures		
	100 °C	130 °C	150 °C
0	3.18	3.25	3.25
0.05	3.20	3.28	3.31
0.1	3.22	3.32	3.33
0.3	3.25	3.35	3.36

the Kubelka-Munk function. The value is obtained by extrapolating the tangent to the intersection of $h\nu$ (horizontal axis). The calculated band gap values are tabulated as shown in table 2. The absorption edges of all samples are at ~ 400 nm. In copper-modified TiO₂ samples a small absorption change is observed in the range 400–500 nm. This may be due to the interfacial transfer of charge from the valence band of TiO₂ to Cu on the surface of TiO₂. A strong absorption at 700–800 nm may be due to d-d transitions on copper [16]. The absorption edge slightly shifts to the visible region for Cu-modified M-TiO₂ when compared to pure M-TiO₂. Hence it can be inferred that modifying TiO₂ with copper increases the photo-catalytic activity of M-TiO₂ with visible-light response.

4 Conclusions

In the present study, highly ordered spherical M-TiO₂ with attractive textural properties have been prepared successfully by the hydrothermal method using cationic (CTAB) surfactant. Simple Cu-modification on this M-TiO₂ by the impregnation method induces visible-light absorption through interfacial charge transfer. Structural investigation by XRD confirms the existence of a pure anatase phase before and after surface modification, suggesting that there is no change in the structure of TiO₂ upon Cu modification. Morphological studies reveal that CTAB-assisted M-TiO₂ exhibits a uniform spherical morphology and homogeneity. It was also observed that when the synthesis temperature increases, the particle size also increases because, at a higher temperature, particles get agglomerated and hence make crystal growth increase. Fine distribution of ordered spherical TiO₂ particles with high surface area of MT-150 with respect to pure TiO₂ may be used for enhanced photo-catalytic activity.

The authors would like to thank Koneru Lakshmaiah Education Foundation for their support during the work and Department of Science and Technology for providing the funding under the scheme of Young Scientist, File No: SB/FTP/ETA-0213/2014.

References

1. D.P. Macwan, P.N. Dave, S. Chaturvedi, *J. Mater. Sci.* **46**, 3669 (2011).
2. Y. Liu, Y. Yang, *J. Nanomater.* **2016**, 8123652 (2016).
3. M. Gratzel, *Prog. Photovolt. Res. Appl.* **8**, 171 (2000).
4. A. Fujishima, K. Honda, *Nature* **238**, 37 (1972).
5. A. Zaleska, *Recent Pat. Eng.* **2**, 157 (2008).
6. D.S. Kim, S.Y. Kwak, *Appl. Catal. A* **323**, 110 (2007).
7. L. Li, C.Y. Liu, *J. Phys. Chem. C* **114**, 1444 (2010).
8. H. Wang, Y. Song, W. Liu, S. Yao, W. Zhang, *Mater. Lett.* **93**, 319 (2013).
9. J.C. Yu, L. Zhang, J. Yu, *Chem. Mater.* **14**, 4647 (2002).
10. K.J. Hwang, J.W. Lee, S.J. Yoo, S. Jeong, D.H. Jeong, W.G. Shim, D.W. Cho, *New J. Chem.* **37**, 1378 (2013).
11. Z. Wang, T. Jiang, Y. Du, K. Chen, H. Yin, *Mater. Lett.* **60**, 2493 (2006).
12. Z. Tan, K. Sato, S. Ohara, *Adv. Powder Technol.* **26**, 296 (2016).
13. Y. Wang, W. Duan, B. Liu, X. Chen, F. Yang, J. Guo, *J. Nanomater.* **2014**, 178152 (2014).
14. L.S. Yoong, F.K. Chong, B.K. Dutta, *J. Energy* **34**, 1652 (2009).
15. C. Sangwichien, G.L. Aranovich, M.D. Donohue, *Colloids Surf. A* **206**, 313 (2002).
16. S. Rtimi, *Catalysts* **7**, 57 (2017).